

## Synthesis of hydroxyapatite nanoparticles through inverse microemulsions

*K. Akhavan*<sup>1\*</sup>

<sup>1</sup> *Department of Chemistry, Rasht Branch, Islamic Azad University, Rasht, Iran*

Received: 15 June 2022; Accepted: 18 August 2022

---

**ABSTRACT:** This study is focused on the formation of hydroxyapatite (HA) nanoparticles in an inverse microemulsion processing route, in which cyclohexane is used as the organic phase, cetyltrimethylammonium bromide as surfactant phase, n-pentanol as surfactant, and a solution of  $\text{Ca}(\text{NO}_3)_2$  and  $(\text{NH}_4)_2\text{HPO}_4$  is used as the aqueous phase. The influence of polyelectrolyte sodium salt of poly acrylic acid (PAA) and a reactant concentration on the final structure of HA nanoparticles were investigated. A wide variety of morphologies were encountered in synthesis which produced rod-like particles (10-15 nm in diameter and 40-50 nm in length), nanosphere particles (5-15 nm in diameter), and needle-like particles (20-30 nm in diameter and 100-200 nm in length). A great structural diversity resulted in the presence of PAA and by reactant concentration alteration. Finally, the synthesized nanoparticles were visualized by transmission electron microscopy (TEM) and identified by FT-IR and X-ray.

**Keywords:** *Hydroxyapatite, Inverse microemulsion, Nanoparticles, Polyelectrolyte, Surfactant*

---

## INTRODUCTION

Hydroxyapatite [ $\text{HA}$ ,  $\text{Ca}_{10}(\text{PO}_4)_6(\text{OH})_2$ ] is a principal inorganic constituent of bones and teeth. Synthetic HA has excellent biocompatibility and bioactivity. Therefore, it is useful in the reconstruction of damaged bone or tooth zones. Hydroxyapatite can also be applied in industrial and technological fields such as water purification, fertilizers production, drug delivery and non-viral gene delivery [1-9]. The function of HA is largely influenced by its morphology, crystallinity, and crystal size distribution. Various synthetic

methods, including co-precipitation, hydrothermal reactions, sol-gel synthesis, the pyrolysis of aerosols, and, recently, the microemulsion method, have been used for the preparation of HA nanoparticles. Among these methods microemulsion is one of the most flexible and convenient method and it is able to produce a particle size and morphology in the nano meter scale with minimum agglomeration [10-13]. Microemulsion is defined as the thermodynamically stable, optically clear isotropic dispersions of two immiscible liquids consisting of nano-sized droplets of one liquid in another. In microemulsion, the system is stabilized by a

---

(\*) Corresponding Author - e-mail: kakhavan@iaurasht.ac.ir  
kobra.akhavan@gmail.com

surfactant [14]. Nanoparticle synthesis with the microemulsion method has been a new research topic since the early 1980s. Morphology control and size distribution is the most challenging dilemma in this synthesizing procedure. It has been found that reactant concentrations show a considerable influence on the final particle-size distribution. First, the particle size increases with a reactant concentration for a flexible surfactant film. Second, the particle size decreases as a function of the reactant excess [10]. This phenomenon is explained assuming that the reactant excess implies a faster nucleation that results in smaller particles [15, 16]. Recently, it has vastly been reported that water-soluble polymers (polyelectrolytes) can be incorporated into inverse microemulsion droplets [17, 18]. On the other hand, polyelectrolytes can control the size and the shape of the nanoparticles during the formation process. Therefore, polyelectrolyte-modified microemulsion can be used successfully as a new type of template for the synthesis of nanoparticles with controlled size, shape, and morphology. This paper is focused on investigating change in the morphology of synthesized HA nanoparticles with a reactant concentration and the presence of PAA.

## EXPERIMENTAL

Ca (NO<sub>3</sub>)<sub>2</sub>·4H<sub>2</sub>O, (NH<sub>4</sub>)<sub>2</sub>HPO<sub>4</sub>, NH<sub>4</sub>OH, cyclohexane, n-pentanol, cetyltrimethylammonium bromide, CTAB with 99% purity, and PAA, were purchased from Merck and Fluka. All of the chemicals were prepared with an analytical reagent grade and were used without further purification. All prepared sample solutions had a Ca/P molar ratio equal to 1.67 (the stoichiometric ratio of HA). Na-polyacrylate was used as a commercial product with a low molar mass (MW= 8000 g/mol).

### *Synthesis route A*

HA nanoparticles were prepared in different concentration of reactants (0.5 and 1M of Ca (NO<sub>3</sub>)<sub>2</sub>·4H<sub>2</sub>O, 0.3 and 0.6M of (NH<sub>4</sub>)<sub>2</sub>HPO<sub>4</sub>). After preparing of 0.1M solution of CTAB in 60 ml cyclohexane and 1.6 ml n-pentanol, 1 ml aqueous solution of Ca (NO<sub>3</sub>)<sub>2</sub>·4H<sub>2</sub>O was injected slowly into the CTAB solution. A transparent solution was obtained upon stirring of the sys-

tem for about 15 min. For formation of HA precursors, under stirring, 1ml aqueous solution of (NH<sub>4</sub>)<sub>2</sub>HPO<sub>4</sub> was directly added to the above-mentioned CTAB reverse microemulsion. Then, a small amount of ammonia was added to the system to adjust pH in the range of 9-10. Transparent solution was gained with stirring the system for about 30 min, then age with continuous stirring at room temperature for one day. Finally, a small amount of ethanol was added into the transparent solution to afford the production of white slurry, which was centrifuged to collect the white colloidal HA. The precipitates were rinse with ethanol for three times and dried at 50°C for 24h. Dried products were characterized by XRD (Philips expert pro. with Cu Ka radiation ( $\lambda=0.154$  nm)), Transmission electron microscope (TEM; Philips), and Fourier-transform infrared spectroscopy (FT-IR; Thermo Nicolet Nexus 870).

### *Synthesis Route B*

Route B was carried out similar to route A, but instead of using 1ml of 1M Ca(NO<sub>3</sub>)<sub>2</sub>·4H<sub>2</sub>O aqueous solution, 1ml of 1M Ca (NO<sub>3</sub>)<sub>2</sub>·4H<sub>2</sub>O in 4% (w/v) of polymeric aqueous solution (PAA) was used to prepare HA nanoparticles. This route was carried out only for one concentration of reactants (1M of Ca (NO<sub>3</sub>)<sub>2</sub>·4H<sub>2</sub>O and 0.6 M of (NH<sub>4</sub>)<sub>2</sub>HPO<sub>4</sub>).

## RESULTS AND DISCUSSION

In this study, the influence of two variables, including the presence of polyelectrolyte, PAA, and the concentration of reactants, on morphology of the synthesized HA nanoparticles were investigated. With increasing the reactants concentrations, the morphology of the synthesized HA nanoparticles is changed from rod-like to spherical like shapes and the particle size decreases. Smaller particle size suggests particle growth commencing on a larger number of nuclei. Polyelectrolyte-modified microemulsions seem to be very interesting template phases for the nanoparticles formation due to the special features of the incorporated polyelectrolyte, including polyelectrolyte-surfactant interactions, polyelectrolyte-nanoparticle interactions [13]. In this study, presence of PAA changes the morphology of HA from spherical particles to needle-like

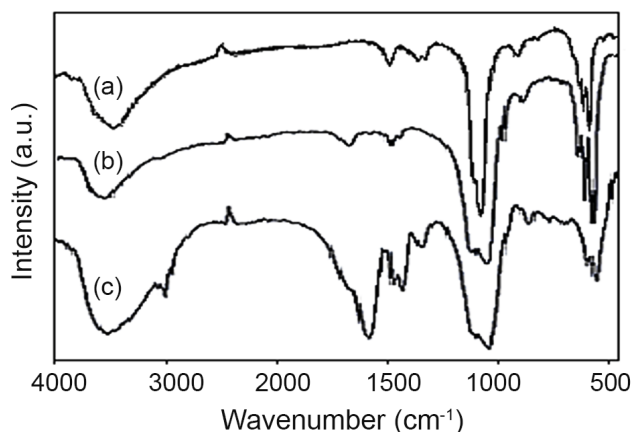


**Fig. 1.** FT-IR spectra of synthesized HA nanoparticles for different molar of  $[Ca^{2+}]$ ; a: 0.5M, b: 1M, and c: 1M and in the presence of PAA.

shapes and increases the particle size of HA nanoparticles. Fig. 1 shows the effect of two various reactant concentrations and presence of polyelectrolyte on the FT-IR spectrum of synthesized HA nanoparticles. In all spectra, the IR characteristic peaks of phosphate groups appears between  $1030-1090$  and  $560-600\text{ cm}^{-1}$  and the absorption bands at  $3420$  and  $1640\text{ cm}^{-1}$  are assigned to the bending mode of the adsorbed water, while the sharp peak at  $3570\text{ cm}^{-1}$  is assigned to the stretching vibration of the lattice  $OH^-$  ions. A medium sharp peak at  $630\text{ cm}^{-1}$  is assigned to the  $OH^-$  group of HA. The weak bands of the  $CO_3^{2-}$  group ( $870$ ,  $1415$ ,  $1450$ , and  $1540\text{ cm}^{-1}$ ) indicated that the  $CO_3^{2-}$  substituting came from a reaction between atmospheric carbon dioxide and high-solution pH ( $>9$ ) [15]. According to the Fig. 1c, there is an increase in the intensity of the absorption bands of  $OH^-$  and  $CO_3^{2-}$  in the presence of Na-Polyacrylate [20-22].

Fig. 2 exhibits the XRD patterns of the produced particles in the microemulsion media in presence of

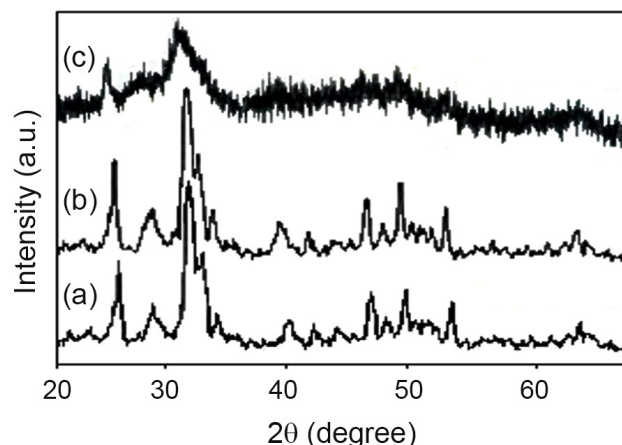


**Fig. 2.** XRD patterns of synthesized HA nanoparticles for different molar of  $[Ca^{2+}]$ ; a: 0.5M, b: 1M, and c: 1M and in the presence of PAA.

PAA and by the variation of the involved reactant concentrations. Using low temperature may cause poor crystalline nature of the prepared HA. The crystallinity of the HA powders synthesized via reverse microemulsion is better than those synthesized via polyelectrolyte-modified microemulsion because the peaks of HA/PAA composite in comparison to the pure HA are broader [23]. No marked different results are gained for various shapes of synthesized HA nanoparticles in diverse reactant concentrations. The XRD and FT-IR proved that the synthesized crystals were HA.

Fig. 3 shows the morphology of HA particles prepared in the microemulsion system in various concentration of aqueous solutions and in the presence of PAA. HA particles are in the form of a rod-like (Fig. 3a), spherical particle (Fig. 3b), and needle-like (Fig. 3c). As the reactant concentrations increase the morphology of nanoparticles shifts from rod-like to sphere-like shapes. It has been observed that the size of rod-like nanoparticles decreases from  $10-15\text{ nm}$  in

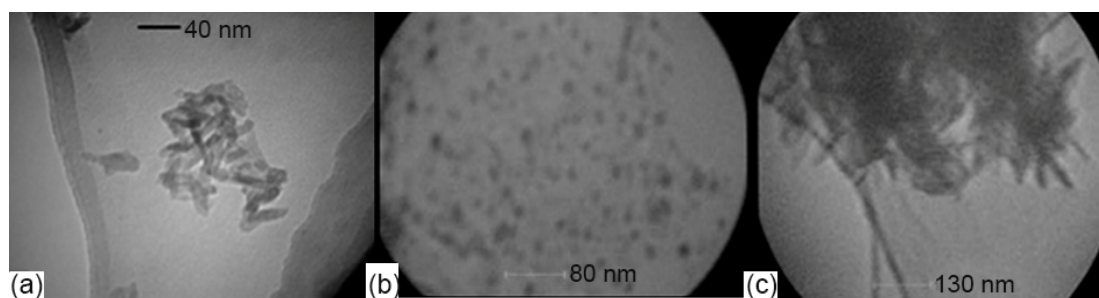


**Fig. 3.** TEM micrographs of synthesized HA nanoparticles for different molar of  $[Ca^{2+}]$ ; a: 0.5M, b: 1M, and c: 1M and in the presence of PAA.

diameter to 5-15 nm in diameter for nanosphere.

In the presence of PAA and with constant reactant concentrations ( $[Ca^{2+}] = 1M$ ,  $[PO_4^{3-}] = 0.6M$ ), the particle size increases from 5-15 nm in diameter for sphere-like shapes to 20-30 nm in diameter and 100-200 nm in length for needle-like shape. Indeed, the morphology of nanoparticles shifts from spherical to needle-like shapes. As mentioned above, reverse micelle could form different morphology in microemulsion depending on reactant concentration and presence of polyelectrolytes [23].

## CONCLUSION

Microemulsions act as the template to control the morphology of nanomaterials. According to the above mentioned experimental results, it could be clearly shown that the size and the morphology of the HA nanoparticles are dependent upon the reactant concentration and presence of PAA. With relatively high reactant concentration, spherical HA or ellipsoidal nanoparticles are predominantly gained. In the presence of PAA, HA nanoparticles with needle like shape could be obtained [17]. However, with lower reactant concentration, rod-like HA nanoparticles could be successfully synthesized. In general, by controlling reactant concentration, we could control the particle size. In the microemulsion system, changing the conditions of the preparation can affect the properties of the products.

## REFERENCES

- [1] Torrent-Burgues, J., Rodriguez-Clemente, R. (2001). Hydroxyapatite precipitation in a semi-batch process. *Cryst Res. Technol.*, 36, 1075–1082.
- [2] Arends, J., Christoffersen, J., Eckert, H., et al. (1987). A Calcium Hydroxyapatite Precipitated from an Aqueous Solution: An International Multimethod Analysis. *J. Crystal Growth*, 84, 515-532.
- [3] Pon-on, W., Meejoo, S., Tang, I.M. (2008). Formation of hydroxyapatite crystallites using organic template of polyvinyl alcohol (PVA) and sodium dodecyl sulfate (SDS). *Mater Chem. Phys.*, 112, 453-460.
- [4] Barroug, A., Glimcher, M.J. (2002). Hydroxyapatite crystals as a local delivery system for Cisplatin: adsorption and release of Cisplatin in vitro. *J. Orthop. Res.*, 20, 274-280.
- [5] Salvador, M., Gutierrez, G., Noriega, S., Moyano, A., Lopez, M.C.B. (2021). Microemulsion synthesis of superparamagnetic nanoparticles for bioapplications. *Mol. Sci.*, 22, 427.
- [6] Tanimoghadam, S., Salabat, A. (2018). A microemulsion method for preparation of thiol-functionalized gold nanoparticles. *Particuology*, 37, 33-36.
- [7] Kazemi, M., Zarandi, M., Monfared, Z.M.R. (2020). Preparation of permanent red 24 nanoparticle by oil in water microemulsion. *Iran J. Chem. Eng.*, 39, 43-49.
- [8] Akhavan, K. (2018). Synthesis of HA nanoparticles in the presence of anionic and cationic polyelectrolyte. *Iranian Chem. Com.*, 6, 49-54.
- [9] Kakizawa, Y., Miyata, K., Furukawa, S. (2004). Size-Controlled Formation of a Calcium Phosphate-Based Organic–Inorganic Hybrid Vector for Gene Delivery Using Poly(ethylene glycol)-block-poly(aspartic acid). *Adv. Mater.*, 76, 699-702.
- [10] Husein, M.M., Rodil, E., Vera, J.H. (2007). Preparation of AgBr Nanoparticles in Microemulsions Via Reaction of AgNO<sub>3</sub> with CTAB Counterion. *J. Nano. Res.*, 9, 787-796.
- [11] Wang, Y.J., Lai, C., Wei, K., Tang, S.Q. (2005). Influence of temperature, ripening time and co-surfactant on solvothermal synthesis of calcium phosphate nanobelts. *Mater Lett.*, 59, 1098–1104.
- [12] Singh, S., Bhardwaj, P., Singh, V., Aggarwal, V.S., Mandal, U.K. (2008). Synthesis of nanocrystalline calcium phosphate in microemulsion-effect of nature of surfactants. *J. Colloid and Interface Sci.*, 319, 322-329.
- [13] Li, H., Zhu, M.Y., Li, L.H., Zhou, C.R. (2008). Processing of nanocrystalline hydroxyapatite particles via reverse microemulsions. *J. Mater. Sci.*, 43, 384–389.
- [14] Tojo, C., Barroso, F. (2011). Surfactant Effects on

- Microemulsion-Based Nanoparticle Synthesis. *Materials*, 4, 55-72.
- [15] Dios, M., Barroso, F. (2009). Simulation of the kinetics of nanoparticle formation in microemulsions. *J. Colloid Interface Sci.*, 333, 741-748.
- [16] Sarkar, D., Tikku, S., Thapar, V., Srinivasa, R.S., Khilar, K.C. (2011). Formation of zinc oxide nanoparticles of different shapes in water-in-oil microemulsion. *Colloids Surf, Physicochem Eng Asp*, 381, 123–129.
- [17] Kotez, J., Bahnemann, J., Lucase, G., Tiersch, B., Kosmella, S. (2004). *Coll. Sur. A: Physicochem. Eng. Aspects*, 250, 423-430.
- [18] Kotez, J., Baier, J., Kosmella, S. (2007). Formation of zinc sulfide and hydroxylapatite nanoparticles in polyelectrolyte-modified microemulsions. *Colloid. Polym. Sci.*, 285, 1719-1726.
- [19] Lim, G.K., Wang, J., Ng, S.C., Gan, L.M. (1996). Processing of Fine Hydroxyapatite Powders. Via an Inverse Microemulsions Route. *Mater. Lett.*, 28, 1431.
- [20] Mollazadeh, S., Javadpour, J., Khavandi, A. (2007). In situ synthesis and characterization of nanosized hydroxyapatite in poly(vinyl alcohol) matrix. *Ceram. Int.*, 33, 1579–1583.
- [21] Wang, Y.J., Chen, J.D., Wei, K., Zhang, SH., Wang, XD. (2006). Surfactant-assisted synthesis of hydroxyapatite particles. *Mater Lett.*, 60, 3227–3231.
- [22] Sinha, A., Guha, A. (2008). Biomimetic patterning of polymer hydrogels with hydroxyapatite nanoparticles. *Materials Science and Engineering C.*, 29, 1330-1333.
- [23] Wang, L., Chunzhong, L. (2007). Preparation and physicochemical properties of a novel hydroxyapatite/chitosan–silk fibroin composite. *Carbohydr. Polym.*, 68, 740-745.

## AUTHORS BIOSKETCHES

**Kobra Akhavan**, Assistant Professor, Department of Chemistry, Rasht branch, Islamic Azad University, Rasht, Iran, *E-mail: kakhavan@iaurasht.ac.ir, kobra.akhavan@gmail.com*